Tetrandrine modulates SQSTM1-mediated selective autophagy and protects pulmonary fibrosis

Yuanyuan Liu¹, Wenshan Zhong¹, Jinming Zhang¹, Weimou Chen¹, Ye Lu¹, Yujie Qiao¹, Zhaojin Zeng¹, Haohua Huang¹, Fei Zou², Xiaojing Meng², shaoxi cai¹, and Hangming Dong¹

¹Southern Medical University Nanfang Hospital ²Southern Medical University

January 28, 2021

Abstract

Background and Purpose Idiopathic pulmonary fibrosis is a progressive fatal disease characterized by interstitial remodeling, with high lethality and a lack of effective medical therapies. Tetrandrine has been proposed to present anti-fibrotic effects, but the efficacy and mechanisms of tetrandrine against lung fibrosis has not been systematically evaluated. We sought to study the potential therapeutic effects and mechanisms of tetrandrine in lung fibrosis. Experimental Approach The anti-fibrotic effects of tetrandrine were evaluated in bleomycin-induced mouse models and TGF- β 1-stimulated murine lung fibroblasts. We performed Chromatin Immunoprecipitation (ChIP), Immunoprecipitation (IP) and mRFP-GFP-MAP1LC3B adenovirus construct to investigate the novel mechanisms of tetrandrine-induced autophagy. Key Results Tetrandrine decreased TGF- β 1-induced expression of α -smooth muscle actin, fibronectin, vimentin and type 1 collagen and proliferation in fibroblasts. Tetrandrine restored TGF- β 1-induced phosphorylated mtOR was inhibited by tetrandrine, with reduced activation levels of Rheb. In vivo tetrandrine suppressed the bleomycin-induced expression of fibrotic markers and improved pulmonary function. Conclusion and Implications Our data suggest that tetrandrine might be recognized as a novel autophagy inducer, thus attenuating lung fibrosis. Tetrandrine should be investigated as a novel therapeutic strategy for IPF.

Tetrandrine modulates SQSTM1-mediated selective autophagy and protects pulmonary fibrosis

Running title: Tetrandrine for the treatment of pulmonary fibrosis

Yuanyuan Liu^{1#}, Wenshan Zhong^{1#}, Jinming Zhang¹, Weimou Chen¹, Ye Lu¹, Yujie Qiao¹, Zhaojin Zeng¹, Haohua Huang¹, Fei Zou², Xiaojing Meng², Shaoxi Cai^{1*} and Hangming Dong^{1*}

¹ Department of Respiratory and Critical Care Medicine, Chronic Airways Diseases Laboratory, Nanfang Hospital, Southern Medical University, Guangzhou, China;

² Department of Occupational Health and Medicine, Guangdong Provincial Key Laboratory of Tropical Disease Research, School of Public Health, Southern Medical University, Guangzhou, China

[#]These authors contributed equally to this work.

Corresponding authors:

Hangming Dong, M.D

Chronic Airways Diseases Laboratory, Department of Respiratory and Critical Care Medicine, Nanfang Hospital, Southern Medical University, Guangzhou, China.

E-mail: dhm@smu.edu.cn

Shaoxi Cai, M.D

Chronic Airways Diseases Laboratory, Department of Respiratory and Critical Care Medicine, Nanfang Hospital, Southern Medical University, Guangzhou, China.

E-mail: caishaox@fimmu.com

Word count: 3409

Acknowledgements: The project was supported by grants the National Natural Science Foundation of China (Grants 81870058 and 81670026).

Conflict of interest statement: The authors declare no conflicts of interest.

Abstract

Background and Purpose

Idiopathic pulmonary fibrosis is a progressive fatal disease characterized by interstitial remodeling, with high lethality and a lack of effective medical therapies. Tetrandrine has been proposed to present anti-fibrotic effects, but the efficacy and mechanisms of tetrandrine against lung fibrosis has not been systematically evaluated. We sought to study the potential therapeutic effects and mechanisms of tetrandrine in lung fibrosis.

Experimental Approach

The anti-fibrotic effects of tetrandrine were evaluated in bleomycin-induced mouse models and TGF-β1stimulated murine lung fibroblasts. We performed Chromatin Immunoprecipitation (ChIP), Immunoprecipitation (IP) and mRFP-GFP-MAP1LC3B adenovirus construct to investigate the novel mechanisms of tetrandrine-induced autophagy.

Key Results

Tetrandrine decreased TGF- β 1-induced expression of α -smooth muscle actin, fibronectin, vimentin and type 1 collagen and proliferation in fibroblasts. Tetrandrine restored TGF- β 1-induced impaired autophagy, accompanied by the up-regulation and enhanced interaction of SQSTM1 and MAP1LC3-II. ChIP studies revealed that NRF2 bound to SQSTM1 promoter in tetrandrine-induced autophagy. Furthermore, TGF- β 1-induced phosphorylated mTOR was inhibited by tetrandrine, with reduced activation levels of Rheb. In vivo tetrandrine suppressed the bleomycin-induced expression of fibrotic markers and improved pulmonary function.

Conclusion and Implications

Our data suggest that tetrandrine might be recognized as a novel autophagy inducer, thus attenuating lung fibrosis. Tetrandrine should be investigated as a novel therapeutic strategy for IPF.

Keywords

pulmonary fibrosis, tetrandrine, autophagy, SQSTM1, mTOR, Col-I

Bullet point summary

What is already known:

Tetrandrine is a drug marketed for the treatment of silicosis

What this study adds:

Tetrandrine attenuates lung fibrosis by activating autophagy

Clinical significance:

Tetrandrine may serve as a potential candidate for the treatment of autophagy-related diseases

Tetrandrine can improve disease progression in lung fibrosis

Introduction

Idiopathic pulmonary fibrosis is a prototype of chronic, progressive, and fibrotic lung disease, characterized by repetitive injury to the lung epithelium, activation and proliferation of (myo)fibroblasts and altered production of extracellular matrix (J, A, R & journal, 2015; TE, A & M, 2011). Despite this high unmet clinical need, only two anti-fibrotic drugs, Pirfenidone and Nintedanib have been approved to date. Moreover, these agents slow, rather than halt, disease progression in IPF (King et al., 2014; Richeldi et al., 2014). Thus, there is a tremendous interest in investigating the pathomechanisms underlying IPF in order to identify novel therapies.

Tetrandrine (TET) is a low-toxicity drug extracted from the plant Stephania tetrandra S. Moore (Fenfangji) of the menispermaceae (Bhagya & Chandrashekar, 2016). Previous studies have reported anti-fibrotic effects of TET in multiple organs, primarily by interfering with autophagy (Wang et al., 2015). Moreover, some demonstrated that TET is an effective broad-spectrum inducer of autophagy and is more potent than rapamycin at activating autophagy [16]. However, the mechanism of TET resolving lung fibrosis and whether TET may be therapeutically used to improve lung function remains largely untested.

Autophagy is a metabolic process which controls the clearance and recycling of intracellular constituents for the maintenance of cellular survival (Barth, Glick & Macleod, 2010) and is known to participate in removing ubiquitinated proteins (Ciani, Layfield, Cavey, Sheppard & Searle, 2003). SQSTM1 is a critical selective autophagy receptor (Lippai & Low, 2014). Recent work has further demonstrated autophagy in many fibrotic diseases. Intriguingly, defective fibroblast autophagic processes have been implicated in the pathogenesis of IPF (Araya et al., 2013; Patel et al., 2012). Transforming growth factor $\beta 1$ (TGF- $\beta 1$) is one of the major profibrotic cytokines for myofibroblast differentiation that could inhibit autophagy in human lung fibroblasts. Loss of autophagy in patients with IPF may potentiate the effects of TGF- $\beta 1$ with respect to extracellular matrix production and transformation to a myofibroblast phenotype. Furthermore, autophagy may contribute to the degradation of COL1/collagen I to inhibit fibrosis (Moscat & Diaz-Meco, 2009; Sosulski, Gongora, Danchuk, Dong, Luo & Sanchez, 2015).

The purpose of the current study was to follow up on previous studies and investigate the role of TET in experimental lung fibrosis and its potential effects on autophagy. We analyzed anti-fibrotic effect of TET in TGF- β 1-induced fibroblast transdifferentiation and bleomycin-induced murine lung fibrosis. We demonstrate that TET therapy decreases fibrotic markers in vitro and in vivo. These effects of TET are associated with autophagy activation, including SQSTM1-dependented degradation of ubiquitinated proteins, NRF2-SQSTM1 axis and Rheb-mTOR signaling. Our findings provide important proof-of-concept evidence for TET activating autophagy as a novel pharmacological approach for treatment of human IPF.

Methods

Culture of Lung Fibroblasts

Primary mouse lung fibroblasts (pMLFs) were isolated from the lungs obtained from C57BL/6J mice and maintained in DMEM supplemented with 10% FBS and penicillin–streptomycin. pMLFs were isolated using a method described previously (Bueno et al., 2015). Briefly, mouse lungs were minced into 1- to 2-mm³ pieces and incubated in calcium- and magnesium-free Hanks' balanced salt solution (HBSS) containing 1,000 U/ml collagenase A for 30 min, and after washing with HBSS, then add 0.25% trypsin-EDTA for 20 min at 37°C with shaking. The dissociated cells were centrifuged and cultured in DMEM supplemented with 10% FBS for

 $1~\rm{h},$ and then adherent fibroblasts were rinsed with HBSS and cultured in DMEM supplemented with 10% FBS and penicillin–streptomycin. More than 95% of the cells were morphologically fibroblasts and stained with vimentin, and no cells were stained with CD45. The fibroblasts were used between culture passages 3 and 6.

Cell viability assay

Cell viability was measured by a cell counting Kit-8 (CCK8) assay (Dojindo, Japan). Cells were seeded in 200 μ L of growth medium at a density of 8x10³ cells per well in 96-well plates. Cells were treated with or without TET for 24h. Following the manufacturer's recommendations, 10 μ L CCK-8 solution was added per well for 2 h before the end of incubation at 37. Cell viability was measured at an absorbance of 450 nm.

Transfection of siRNA and plasmids

Different siRNA oligos were obtained from Gene Pharma (Shanghai, China), and the sequences were listed in Supplementary Table 1. Plasmids for Rheb overexpression were purchased from Hanbio (Shanghai, China) and the sequence is shown in Supplementary Table 1. Cells were transfected with the appropriate siRNA oligos or plasmid with Lipofectamine 3000 (Invitrogen, CA, USA), according to the manufacturer's protocol. After 48h, cells were further stimulated with different reagents. The successfully transfected clones were confirmed by western blotting.

Tandem fluorescent-mRFP-GFP-MAP1LC3B-denovirus transduction of pMLFs

pMLFs were transfected with a tandem fluorescent-mRFP-GFP-MAP1LC3B-adenovirus (HanBio, HB-AP2100001) that expresses a specific marker of autophagosome formation to detect autophagy, according to the manufacturer's instructions (Hariharan, Zhai, Sadoshima & signaling, 2011). With this tandem construct, autophagosomes and autolysosomes are labelled with yellow (mRFP and GFP) and red (mRFP only) signals, respectively. Five fields were chosen from 3 different cell preparations. GFP- and mRFP-expressing spots, which were indicated by fluorescent puncta and DAPI-stained nuclei were counted manually. The number of spots per cell was determined by dividing the total number of spots by the number of nuclei in each field.

Immunofluorescence assay

The immunofluorescence assay was performed as described previously (Ohashi et al., 2015). Cells were seeded on a confocal dish for 24h. After treatment, cells were fixed with 4% paraformaldehyde for 15 min in phosphate-buffered saline (PBS), followed by permeabilization for 10 min with Triton X-100–containing buffer. Antibodies was used for immunofluorescence assays. Cells were washed with PBS, and incubated with Alexa Fluor 594 anti-Rat (1:200) and Alexa Fluor 488 anti-mouse (1:200) (Life Technologies, CA, USA) at room temperature for 2 h afterwards. The nuclei of the cells were stained with DAPI (Invitrogen). Images were taken on an Olympus FV1000 Confocal Laser Scanning Microscope (Tokyo, Japan). The following antibodies were used: MAP1LC3B (CST, 2775s, 83506S), SQSTM1 (proteintech, 18420-1-AP, 66184-1-AP), Anti-alpha smooth muscle Actin (Abcam, ab7817), Cleaved caspase-3 (CST, 9664s), ubiquitin (Proteintech, 10201-2-AP), Phospho-4E-BP1 (Thr37/46) (236B4) (CST, 2855T), LAMP2 (Abcam, Ab13524), Collagen1 (Affinitiy, AF7001).

Network Pharmacology and Bioinformatics Analysis

Pulmonary fibrosis-related genes were obtained from the the Comparative Toxicogenomics Database (CTD, http://ctdbase.org/) and DisGeNET (a database of gene-disease associations, https://www.disgenet.org/) using the term "pulmonary fibrosis, followed by filtering with the term "Homo sapiens". Potential targets of TET were obtained from the Swiss target prediction, (http://www.swisstargetprediction.ch/) and pubchem (https://pubchem.ncbi.nlm.nih.gov/). A total of 74 potential human targets were obtained and the official gene names were obtained from Uniprot (http://www.uniprot.org/) by confining the species to "Homo sapiens". Subsequently, various ID forms of the targets were transformed into UniProt IDs. The Search Tool for the Retrieval of Interacting Genes (STRING) database (https://string-db.org/) supplies each predicted

PPI information as well as the data which have actually been experimentally confirmed. Then, we seek out the intersection through Cytoscape- Bisogenet (3.7.2) and screen out the top ten key genes. The functional pathways of TET related to pulmonary fibrosis were analyzed using the Kyoto Encyclopedia of Genes and Genomes (KEGG) pathway and gene ontology (GO) enrichment evaluation based upon the database for annotation, Visualization and Integrated Discovery (DAVID) version 6.8 (https://david.ncifcrf.gov/). P-value was calculated in these two enrichment analyses, and P < 0.05 suggests the enrichment degree was statistically significant and the pathway results would certainly be necessary functional mechanisms of pulmonary fibrosis.

Western blotting and Co-immunoprecipitation

Total cell lysates were obtained using the Total Protein Extraction Kit (KeyGen Biotech, China) according to the manufacturer's instructions. Proteins were subjected to SDS-PAGE, transferred to PVDF membranes, and probed with various primary antibodies and LICOR: fluorescence-labeled secondary antibodies (#926-68071, 926-32210). Blots were visualized using Odyssey finally. For co-immunoprecipitation, protein extracts from MLFs were incubated with indicated primary antibody overnight at 4°C. The immune-complexes were cleared with Protein A/G Magnetic Beads (Thermo Scientific). Input lysates were run simultaneously with the IP samples on 10% polyacrylamide gels and visualized with LICOR. Antibodies used were: anti- β -actin (Proteintech, 66009-1-Ig), anti-phospho-mTOR (Ser2448; Cell Signaling Technology, 5536S), anti-Phospho-P70 (Thr389; Cell Signaling Technology, 9236S), anti-Phospho-4E-BP1 (Thr37/46; Cell Signaling Technology, 2855T), anti-phospho-smad3 (Ser423/425; Cell Signaling Technology, 9520T), anti-phospho-smad2 (Ser465/Ser467; Cell Signaling Technology, 18338T), anti-MAP1LC3-I/II (Cell Signaling Technology, 2775S), anti-cleaved caspase3 (Cell Signaling Technology, 9664S), anti- α -SMA (Abcam, ab32575), anti-fibronectin (Abcam, ab2413), Anti-Rheb (Santa Cruz, sc-271509), anti-SQSTM1 (Proteintech, 18420-1-AP), anti-4E-BP1 (Proteintech, 60246-Ig), anti-p70(S6K) (Proteintech, 14485AP), anti-mTOR (Proteintech, 20657-1-AP), anti-ATG7 (Proteintech, 10088-2-AP), anti-vimentin (Proteintech, 10366-1-AP), anti-IgG (Proteintech, B900610), anti-smad3 (Proteintech, 25494-1-AP), anti-smad 2 (Proteintech, 12570-1-AP), anti-Col-I (Affinity, AF7001). Ubiquitin (Proteintech, 10201-2-AP)

Chromatin Immunoprecipitation (ChIP) Assay

The immunoprecipitation (ChIP) assay in MLFs was performed using the SimpleChIP Enzymatic Chromatin IP Kit (CST, 9003) according to the manufacturer's protocol. Approximately 4×10^6 cells were used for each immunoprecipitation. Chromatin was immunoprecipitated with the immunoglobulin G (CST, #2729; as a negative control) or NRF2(Genetex, #GTX103322). In all, 10% total DNA was used for input evaluation. DNA enrichment in the ChIP samples was determined by Reverse transcription and semi-quantitative PCR (RT-PCR) with PrimeScript RT reagent Kit with gDNA Eraser (Takara, China) and a LightCycler 96 Instrument (Roche) following the manufacturer's protocol. PCR products of immunoprecipitated and input samples were analyzed on a 2% agarose gel. Specific primer sets for the SQSTM1 locus are shown as follow: SQSTM1_P1 forward: ATTCTGCCCTGCATGTCTT, reverse: GCCTTCTAGGTATGGTCCTTTC; SQSTM1_P2 forward: TGGCCGAGCCTTGAATTAG, reverse: GCACCTGCCTAGTATGTGTT.

RNA extraction and quantitative real-time PCR

Total RNA was extracted from cells with the TRIzol reagent (Takara, Dalian, China). The quantity and quality of RNA were determined using a Nanodrop 2000 spectrophotometer (Thermo Fisher Scientific), and then RNA was reverse transcribed using iScript cDNA synthesis kit (Biorad; 1708890) according to the manufacturer's instructions. The qPCR was performed using TaqMan(r) Universal PCR Master Mix (Fisher Scientific; 4304437) on a StepOnePlus Real-Time PCR System (Thermo Fisher Scientific) in 20 μ L reaction. Relative mRNA levels were calculated using the 2^{-CT} method normalized against β -actin in each reaction. The following primers were used, Actb, forward: GTGACGTTGACATCCGTAAAGA, reverse: GCCGGACTCATCGTACTCC; SQSTM1, forward: ATGTGGAACATGGAGGGAAGA, reverse: GGAGTTCACCTGTAGATGGGT; Rheb, forward: GGTCTGTGGGAAAGTCCTCAT, reverse: GGT-GAACGTGTTCTCTATGGTT.

Bleomycin-induced lung fibrosis model and treatment with tetrandrine

All animal experiments were conducted according to Southern Medical University Animal Welfare, and research protocols were approved by the Institutional Animal Care and Use Committee of Southern Medical University. Mice were housed four mice per cage in a specific pathogen-free room with a 12h light/dark schedule at $25^{\circ}C \pm 1^{\circ}C$ and were fed an autoclaved chow diet and water ad libitum. An established mammalian model of idiopathic pulmonary fibrosis (IPF) was utilized as described in previous publications. Six- to eight-week-old C57BL/6 female mice(16-20g) were anesthetized (2,2,2-tribromoethanol, Sigma-Aldrich) and then injected intratracheally with prepared bleomycin sulfate (5 U kg⁻¹) (Hanhui pharmaceuticals co.LTD) in sterile PBS (volume was varied between 80 and 100 µL depending on the body weight). Control mice were injected with 100 µL of sterile PBS. Body weights were monitored throughout each study. Each experimental group consist of at least 5 animals.

To quantitate fibrosis during longitudinal studies, lungs were harvested at 21 days after bleomycin instillation and assayed as described below. To test the prevention efficacy of TET in our modeling of IPF, TET (20mg kg⁻¹, Sigma-Aldrich) or vehicle (equal volume of 0.1% sodium carboxymethyl cellulose) were administered by intraperitoneal injection at every other day after bleomycin administration, and the mice were sacrificed at day 21. For delayed therapy studies, induction of IPF was initiated as described above, and TET (20mg kg⁻¹ or 40mg kg⁻¹) was intraperitoneally injected every other day beginning on day 8. Lungs were harvested on day 21 and assayed as described below (day 0 was taken as the day of bleomycin administration).

Pulmonary function assay

At endpoint, at least 5 mice from each group were anesthetized with 2,2,2-tribromoethanol in saline, tracheotomized below the larynx, and intubated with a tracheal cannula. After the surgery, the mice were placed inside the plethysmographic chamber and the cannula was connected to the machine. Pulmonary function was measured by pulmonary function test system (BUXCO, USA). The system's software automatically records and displays the pulmonary function parameters.

Immunoanalysis and histopathology

Formalin-fixed, paraffin-embedded (FFPE) tissue blocks obtained from mouse models were sectioned at 5 mm. For immunohistochemistry, the FFPE unstained slides were deparaffinized through standard methods. Paraffin embedded sections of mouse lung tissue were pretreated in citrate buffer pH6 for 20 minutes for antigen retrieval. Sections were then incubated with corresponding antibodies. For murine fibrosis assessment, FFPE lung tissue blocks were sectioned at 5 mm and subjected to haematoxylin and eosin and Masson's trichrome staining. Sections were reviewed by a blinded pathologist and approximately half of the specimens were scored by a second blinded pathologist to confirm agreement. Specimens were scored according to an eight-tier, modified Ashcroft scale (Hübner et al., 2008).

Hydroxyproline Assay

Lung hydroxyproline content was analyzed using a hydroxyproline assay kit (#A030-2, Nanjing Jianchen Bioengineering Institute, China) according to the manufacturer's instructions.

Materials

Dimethyl sulfoxide (DMSO) and chloroquine (CQ) were obtained from Sigma-Aldrich (St. Louis, MO, USA). TGF- β 1 were purchased from R&D Systems, Inc. (Minneapolis, MN, USA). 3-Methyladenine (3MA) and MHY1485 were purchased from MedChemExpress (USA).

Data and Statistical Analysis

All data were analyzed blinded and presented as scatter plots showing each single data point representing the number of independent values and means \pm SEM using bars and whiskers. Group sizes in the animal experiment were n[?]5. The number of included data per group was mentioned in the figure legends. After testing values for normal distribution using Kolmogorov-Smirnov test, data were analyzed by: 1) Two-tailed t tests for comparison of two group means, using nonparametric analysis (Wilcoxon or Mann-Whitney) for n=5; 2) One-way analysis of variance (ANOVA) followed by Dunnett's multiple comparisons test was used for multiple comparisons to control for concentration of TET dose effects; 3) Two-way ANOVA followed by Tukey post hoc tests for three or more group means with two factors. Non-parametric data were analyzed by Dunnett's multiple comparison test. Post hoc tests were run only if F achieved Pi0.05 and there was no significant variance in homogeneity. Differences between group means were considered statistically significant at the level of Pi0.05. Statistical analysis was performed using GraphPad Prism 8 for Windows software (version 8.4.2, GraphPad software Inc., San Diego, CA, USA). The data and statistical analysis comply with the recommendations on experimental design and analysis in pharmacology (Curtis et al., 2018).

Results

Τετρανδρινε ινηιβιτς ΤΓΦ-β1-ινδυς
εδ μψοφιβροβλαστς διφφερεντιατιον, προλιφερατιον ανδ Ε
 ${\rm M}$ δεποσιτιον

Fibroblast transdifferentiation is critical pathogenesis processes in IPF (Baek et al., 2012). Previous studies have reported anti-fibrotic effects of TET (chemical structure shown in Figure 1A) in multiple organs (Teng et al., 2015; Yin, Lian, Piao & Nan, 2007). However, whether TET is capable of deactivating differentiated myofibroblasts and resolving fibrosis is not well known. We confirmed that 50% inhibition of cell growth was not achieved until TET concentration at 16 μ M in primary mouse lung fibroblasts (pMLFs) or 32 μ M in IMR90 cells (Figure 1B, Figure S1A). Western blots and Immunofluorescence (IF) revealed that fibronectin, collagen type I, vimentin and α -SMA were all increased in pMLFs and IMR90 cells by stimulation with TGF- β 1 were blocked by co-administration of TET (Figure 1C-F, FigureS1B-E). Moreover, Numbers of *EdU* (+) cells after TGF- β 1 exposure were significantly reduced by TET treatment for pMLFs (Figure 1G-H). TGF- β 1-induced Smad2/3 activation indicated by Smad2/3 phosphorylation was blocked by TET in pMLFs (Figure 1I-K). Taken together, these results suggest that TET suppresses fibroblast transdifferentiation.

Potential Target Genes and Network Analysis of TET Treatment for Pulmonary Fibrosis

To elucidate the potential anti-fibrotic mechanisms of TET, we conducted an integrated systems pharmacology approach as previously described (Klionsky, Cuervo & Seglen, 2007). We compared the respective gene-expression profiles of TET (from LINCS) to that of IPF and identified 74 target genes in IPF lungs visualized using Cytoscape. (Figure 2A). Ten hub genes (AKT1, mTOR, Foxo3, Beclin1, MAP1LC3B, ATG5, ATG7, Rptor, ATG12 and ULK1) were identified in protein-protein interaction (PPI) networks (Figure 2B). We performed GO and KEGG pathway enrichment analysis of above gene sets using Cytoscape. The top enriched biological process is cell metabolism and the top cell component is membrane composition (Figure 2D). Interestingly, PI3K/AKT signaling, apoptosis, and autophagy are the top enriched gene ontology terms in KEGG pathway enrichment analysis (Figure 2C-E). Thus, the above data suggest that TET may relieve pulmonary fibrosis by regulating apoptosis and/or autophagy pathway.

Tetrandrive restores $T\Gamma\Phi$ -b1-induced impaired autophary in $M\Lambda\Phi$ s

To test whether TET regulates autophagy pathway in lung fibrosis, we administered TET to TGF- β 1induced MLFs and evaluated the extent of autophagic flux. Conversion of MAP1LC3-I to MAP1LC3-II was decreased in fibroblasts by stimulation with TGF- β 1, indicating impaired autophagy. The effects of TGF- β 1 were reversed by co-administration of TET in a dose-dependent manner (Figure 3A-B). Interestingly, TET mediates a marked increase in TGF- β 1-induced protein and mRNA expression of SQSTM1 (Figure 3A-D), which indicated TET regulated SQSTM1 in both autophagy dependent and independent manner. We then cotreated the TGF- β 1-induced fibroblasts with TET and autophagy inhibitors 3MA (which blocks early induction of autophagy) or chloroquine (CQ, which blocks fusion of autophagosomes and lysosomes). TET-induced MAP1LC3-II and SQSTM1 expression was inhibited by 3MA, while increased by CQ in TGF- β 1-induced pMLFs (Figure 3E-H). Similarly, Immunofluorescence results indicated that the TET-induced punctate staining of MAP1LC3B was significantly increased after treatment with CQ, and the effect of TET was suppressed by 3-MA in TGF- β 1-treated fibroblasts. (Figure 3I-J). Transmission electron microscopy (TEM) further supported the induction of autophagy by TET in TGF- β 1-stimulated fibroblasts (Figure 3K). To further demonstrate whether TET restores TGF- β 1-induced impaired autophagy, a double tagged MAP1LC3 (mRFP-GFP) plasmid was used to examine autophagic flux. Notably, consistent with rapamycin (RAP, a representative autophagy promotor), TET treatment reduced colocalization of green with red fluorescence (yellow; autolysosomes) and increased red fluorescence (autolysosomes), whereas CQ treatment accumulated yellow fluorescence (autophagosomes) in TGF- β 1-induced MLFs (Figure 3L-M).

In order to validate the relevance of TET with apoptosis in lung fibrosis, we examined the expression of cleaved-caspase3. The results show that TET did not affect the expression of cleaved-caspase3 (Figure S2A-E). Additionally, TET did not induce apoptosis as shown on flow cytometry and TUNEL assay (Figure S2F-H). These findings indicated that TET did activate autophagic flux characterized by SQSTM1 accumulation.

Tetrandrine activates SQSTM1-Mediated Selective Autophagy

The prevailing view is that ubiquitin-tagged misfolded proteins are assembled into aggregates by SQSTM1 (selective autophagy receptor), and the aggregates are then engulfed and degraded by autophagolysosomes (Svenning & Johansen, 2013). Interaction between selective autophagy receptors and MAP1LC3B, is the molecular basis for selective autophagy. We next test whether TET induce autophagy in a SQSTM1 dependent manner. Our IP results show that TET treatment enhanced interaction of SQSTM1 and MAP1LC3B in TGF-β1-induced fibroblast. (Figure 4A-B). Furthermore, the binding of SQSTM1 to ubiquitylated protein was significantly increased by TET (Figure 4C). Similarly, TET treatment efficiently enhanced the colocalization of SQSTM1/MAP1LC3B-positive puncta and induced the SQSTM1-recruited cargos to autophagosomes (Figure 4D-E). Together, TET positively regulates selective autophagy targeting SQSTM1.

NRF2 regulates SQSTM1 transcription involving in TET-induced selective autophagy

Having demonstrated that both protein and mRNA expression of SQSTM1 were increased by TET, partially independent of autophagy pathway, we aim to investigate how TET regulates SQSTM1. Previous research suggested that transcription factor NRF2 can bind to promoter of SQSTM1, leading to promoting SQSTM1 transcription. We found that expression of NRF2 was decreased by TGF-β1, but increased by cotreated with TET in fibroblasts (Figure 5A-B). To further confirm that SQSTM1 is regulated by NRF2, we performed ChIP for endogenous NRF2 in primary MLFs and analyzed the enrichment of NRF2 at the transcription start site (TSS). Firstly, using NCBI website and JASPAR programs, we analyzed the SQSTM1 promoter sequence to identify predicted transcription factor binding sites (Figure 5C-D). Our data show that TET increased enrichment for NRF2 at binding sites of SQSTM1 in TGF-β1-stimulated fibroblasts (Figure 5E-F).

Tetrandrine Activated SQSTM1-Mediated Selective Autophagy via Rheb-mTOR Signaling

The mTOR kinase is a key regulator of autophagy induction(Hu et al., 2015). As our results shown TET significantly suppressed TGF- β 1-induced mTOR activation by dephosphorylating P70 and 4E-BP1. (Figure 6A-D). Similarly, mTOR inhibition by TET was confirmed by immunofluorescent staining (Figure 6E-F). To investigate the role of mTOR during TET-induced autophagy, fibroblasts were treated with MHY1485, an activator of mTOR, after TET stimulation. Importantly, TET enhanced conversion of MAP1LC3-I to MAP1LC3-II, and this effect was reduced by MHY1485 (Figure 6G-I), identifying mTOR signaling as a required upstream event in TET-induced autophagy.

Previous studies suggest mTOR activation is regulated by Rheb, a Ras-like small guanosine triphosphatase (GTPase)(Narita et al., 2011; SM et al., 2011). However, both the total Rheb protein and mRNA expression was not reduced by TET (Figure 6J-L). We next determined the Rheb states by Co-IP. Our results showed that TET reduced Rheb activity in TGF- β 1-stimulated fibroblasts (Figure 6M-N), suggesting TET negatively regulates Rheb activity but not protein or mRNA expression. Taken together, TET activated autophagy through Rheb-mTOR signaling.

Τετρανδρινε αττενυατες $T\Gamma\Phi$ -β1-ινδυς
εδ μψοφιβροβλαστς διφφερεντιατιον ανδ προλιφερατιον β
ψ Ινδυςινγ Αυτοπηαγψ ιν ιτρο

To further examine whether autophagy induction contributes to TET-mediated protective effects in lung fibrosis, we performed pharmacological and transgenic approaches to inhibit autophagy and detected fibrotic markers. The addition of Rapamycin (as a positive control), which induce autophagy, shows downregulation of fibrotic markers in fibroblasts stimulated by TGF- β 1 (Figure 7A-B). These results support that autophagy inducers can attenuate lung fibrosis. We observed that fibronectin, collagen type I, vimentin and α -SMA were all decreased by TET in TGF- β 1-induced fibroblasts, and this effect was blocked by CQ (Figure 7C-F). Furthermore, silencing of ATG7 mediates a marked increase in TET-inhibited expression of fibroblasts transdifferentiation, we overexpress Rheb. The effects of TET on suppressing fibrotic markers induced by TGF- β 1 is lost when Rheb is overexpressed (Figure 7H, Figure S3). Additionally, TET reduced TGF- β 1-stimulated fibrotic expression, in particular induced by MHY1485, a small molecule activator of mTOR (Figure 7I, Figure S3). Taken together, TET attenuates lung fibrosis through inducing autophagy.

Type I Collagen is Degraded by TET-induced Autophagy

As shown before, TET presented a significant decrease in the steady-state levels of collagen inducing by TGF- β 1. However, the mechanism is unknown. Since previous data indicated that intracellular Col-I could degrade by lysosome(Sosulski, Gongora, Danchuk, Dong, Luo & Sanchez, 2015) we hypothesized that Col-I is degraded by autophagy. The addition of TET increased the appearance of lysosomes and the colocalization of Col-I and lysosomes in TGF- β 1-stimulated fibroblasts, indicating lysosomal degradation of Col-I (Figure 8A). Similarly, there are more endogenous Col-I colocalized with autophagosomes in cells treated with TET after TGF- β 1 stimulation (Figure 8B), further confirming that Col-I is degraded by autophagy. Interestingly, TET improved interaction of MAP1LC3B and SQSTM1 in TGF- β 1-induced fibroblasts (Figure 8C). These results suggest that Col-I is delivered to the lysosome via SQSTM1 for degradation during TET-induced autophagy.

TET attenuates lung fibrosis in bleomycin-induced mouse models through activating autophagy

TET is a safe and widely used agent for silicosis, and has therapeutic potential to restore cell metabolic homeostasis(Zhang, Liu, Yu, Li & Li, 2018). We explored whether TET, via autophagy activation, can accelerate the resolution of fibrosis in the bleomycin lung fibrosis model. We examined the effects of TET prevented treatment (20 mg kg⁻¹, intraperitoneally (i.p.)), that is, 1 day after bleomycin injury for up to day 21(Figure 9A). Notably, TET attenuated BLM-induced body weight loss and impaired pulmonary function (Figure 9B-F). TET therapy resulted in significantly lower pulmonary fibrosis as assessed by lower histologic evidence of fibrosis, Masson Trichrome staining and hydroxyproline levels (Figure 9G-J). Histology and immunohistochemistry show diminished amounts of collagen and α -SMA (Figure 9K). Consistent with the histological analysis, immunoblotting show that TET blocked the increase of extracellular matrix (ECM) deposition and α -SMA protein in BLM-challenged mice (Figure 9L-M). Importantly, these effects of TET are accompanied with autophagy activation (Figure 9L).

We also examined the effects of delayed TET treatment (20 and 40 mg kg-1, i.p.), starting on day 8 postbleomycin lung injury (Figure S4A). The results demonstrated significant reductions in several pro-fibrotic markers, including total lung hydroxyproline, histologic change, ECM deposition and weight loss (Figure S4B-F). These data indicated that TET activated autophagy to blunt bleomycin-induced lung fibrosis, suggesting a further potential therapeutic effect of TET on pulmonary fibrosis.

Discussion

Tetrandrine, originally isolated from Chinese herbs but now produced synthetically, has been tested in clinical trials and found effective against silicosis and lung cancer. However, whether tetrandrine has antifibrotic activity and its potential mechanisms has not been systematically evaluated. In this study, we provide evidences that TET can attenuate myofibroblast differentiation, proliferation and ECM deposition, thereby resolving pulmonary fibrosis. We found that TET can enhance the interaction of SQSTM1 with MAP1LC3-II and ubiquitinated proteins, which due to NRF2-mediated SQSTM1 transcription and RhebmTOR signaling activation, thus dramatically induce SQSTM1-selective autophagy, directly leading to Col-I degradation in lysosome (Figure 10). This is the first report to show the potential new mechanisms involving in TET-induced selective autophagy in the context of lung fibrosis.

TET therapy significantly attenuated experimental lung injury and produced similar therapeutic results in animal models of cardiac and liver injury. Although recent report found that inhalation of TET alleviated inflammation and pulmonary fibrosis in a mouse model, starting TET therapy from day 1, evidence in support of its therapeutic utility in IPF was not strengthened. Our results further establish a role for TET in experimental lung fibrosis: TET therapy effectively improved pulmonary function and decreased fibrotic and extracellular matrix markers in two mouse models. Specially, a beneficial effect is observed when TET therapy is initiated during the established fibrosis phase, suggesting enhanced resolution of fibrosis. Similarly, TET inhibits TGF- β 1-induced fibroblast transdifferentiation, proliferation and ECM deposition in vitro. Impressively, TET therapy did not induce apoptosis, in contrast with previous studies(Liu, Gong, Mao & Li, 2011), which might because the TET dose we used is not high to 30μ M and we suggest a more safe and effective concentration in lung fibrosis.

Network pharmacology studies emphasize the paradigm shift from "one target, one drug" to "network target, multicomponent therapeutics," highlighting a holistic thinking also shared by traditional Chinese medicine (TCM) (Li, Fan, Jia, Lu & Zhang, 2014). Through network pharmacology analysis we found that the anti-fibrotic effect of TET may be mediating autophagy. Previous studies using lung biopsies from IPF patients reported a diminution in autophagy (Araya et al., 2013; Patel et al., 2012) and TGF- β 1-mediated regulation of the autophagic response during lung fibrosis is a part of the pathological response to injury and fibrogenesis (Sosulski, Gongora, Danchuk, Dong, Luo & Sanchez, 2015). Herein, we impart an appreciation for tetrandrine-mediated regulation of the autophagic response in TGF- β 1-induced MLFs. Our findings demonstrated that tetrandrine may restrain transdifferentiation of lung fibroblasts and ECM deposition through increasing autophagy flux. Tetrandrine promotes autophagy, in part, by activation of SQSTM1-dependent selective autophagy in lung fibroblasts. Furthermore, tetrandrine increased autophagy flux, MAP1LC3-II/SQSTM1 dependent Ubiquitinated protein recycling and lysosome degradation of Col-I. This study connects autophagy and protein homeostasis to lung fibrosis. Nevertheless, the redundancy of mechanism of tetrandrine that regulate lysosome homeostasis need to be investigated, as protein metabolism is a complex process that involves multiple interacting signaling pathways (Araya & Nishimura, 2010).

SQSTM1 serves as multifunctional regulator of cell signaling involved in selective autophagy (Lamark, Svenning & Johansen, 2017; Lane, Svenning & Johansen, 2013). Both MAP1LC3-II and SQSTM1 are required to activate autophagy in terms of autophagosome formation and the translocation of ubiquitinated proteins to autophagic vesicles, respectively. Interestingly, TET treatment significantly increase protein levels of SQSTM1 and MAP1LC3-II in TGF- β 1-induced MLFs. In addition, CQ, a lysosome inhibitor, can further increase protein levels of SQSTM1 at present of TET. This observation indicates that the increase in SQSTM1 by TET is likely to occur at the transcription level or translation level, rather than due to the SQSTM1 protein accumulation as a consequence of autophagic inhibition. The increase in SQSTM1 expression by TET seemed to be autophagy-independent manner, but could positively contribute to the TET-induced autophagic flux. Previous studies suggest that TGF- β 1-induced mLFs. Emerging studies demonstrate NRF2 binds to the antioxidant response element (ARE) of the SQSTM1 promoter, leading to increasingly SQSTM1 transcription (Liu, Kern, Walker, Johnson, Schultz & Luesch, 2007).

NRF2, a critical transcription factor, has a major anti-oxidant and anti-inflammatory effect. During stress conditions, NRF2 is liberated from the Keap1 protein and translocates into the nucleus to regulate target genes through binding to ARE in their promoters (Hayes & McMahon, 2009; Iso, Suzuki, Baird, Yamamoto & biology, 2016). However, the interaction mechanisms of NRF2 and SQSTM1 is not confirmed in lung fibrosis. We show TET promotes a positive interrelationship between NRF2 and SQSTM1. Our findings implicate that TET can execute its anti-fibrosis effect via NRF2 pathway to increase SQSTM1 levels in

lung fibrosis. Besides, defects in SQSTM1 may contribute to the deregulation in NRF2 activity seen in myofibroblasts and pulmonary fibrosis (Bian et al., 2018; Ichimura et al., 2013). Thus, up-regulation of SQSTM1 by TET may provide dual protection to TGF- β 1-induced MLFs through facilitating both selective autophagy and the NRF2-mediated antioxidant response. However, further investigations are required to clarify the involvement of NRF2 in the SQSTM1 transcription.

The Ras homolog enriched in the brain gene (Rheb) is ubiquitously expressed in mammalian cells and encodes proteins that play an important role in regulating cell growth and survival (Bai et al., 2007). Rheb exists either in an active GTP-bound state or an inactive GDP-bound state and only Rheb-GTP activates the rapamycin complex 1 (TORC1) (SM et al., 2011). Rheb/ mTORC1 signaling plays a critical role for fibroblast activation in kidney fibrosis (Jiang et al., 2013). Our results show that TET can promote conversion of Rheb-GTP to Rheb-GDP, resulting in mTORC1 dephosphorylation. Rheb activates mTOR signaling via several downstream substrates, including p70S6K and eukaryotic translation initiation factor 4E-binding protein 1 (4E-BP1) (Huang & Manning, 2008). Some studies provide strong support that mTORC1 mediates TGF- β 1-induced fibrotic effects through 4E-BP1-dependent manner (Jiang et al., 2013). Indeed, TET inhibit mTORC1- 4E-BP1 signaling in TGF- β 1-induced MLFs. Based on above data, we demonstrate that TET decreases collagen deposition induced by TGF- β 1, partially through mTORC1/ 4E-BP1 signaling.

On the other hand, the inactivated mTORC1 promotes autophagy initiation via phosphorylation-dependent activation of ULK1/2 and the VPS34 complex (Yu et al., 2010). In this section, our data indicate TET can induce autophagy by inhibiting mTORC1 signaling pathway. Although mTORC1 is inactivated during autophagy initiation, it can be reactivated by energy supplies by the degradation of autolysosomal products at the end of autophagy flux. Interestingly, we found that TET can significantly increase the number of lysosomes which might because of mTORC1 reactivated. Its reaction is required for the reformation of functional lysosomes (Yu et al., 2010). Previous studies suggest that mTORC1 directly phosphorylates TFEB, a master transcriptional regulator of lysosomal and autophagy genes (Settembre et al., 2011). Taken together, TET induces autophagy by inactivating mTORC1 to supply more energy, then might reactivates mTORC1 in time-dependent manner to improve lysosome cycle. This part needs further experimental data to support.

Additionally, emerging studies indicate that Col-I can undergo intracellular degradation via autophagy [61]. We provide evidence TET improve co-localization Col-I with LAMP2 and MAP1LC3-II. Among these, we suggest TET reduced Col-I accumulation by dragging Col-1-LC3 complex into the lysosome for degradation. Therefore, TET may improve pulmonary fibrosis partially by promoting the LC3-mediated degradation of Col-I.

In summary, TET, a monomeric component of traditional Chinese medicine, ameliorates BLM-induced experimental lung fibrosis. Besides, we evaluated the antifibrotic effects of TET on both MLFs and IMR90 and reveal that the underlying mechanism of TET involves SQSTM1-mediated selective autophagy via the Rheb/mTORC1 dependent pathway. Furthermore, TET can promote SQSTM1 transcription by NRF2. This study shows a novel mechanism that NRF2 and SQSTM1 play fundamental roles through regulating autophagy in lung fibrosis. Based on these findings, TET should be considered as a therapeutic option for IPF patients.

Availability of data

The data that support the findings of this study are available from the corresponding author upon reasonable request. Some data may not be made available because of privacy or ethical restrictions.

Declaration of transparency and scientific rigour

This Declaration acknowledges that this paper adheres to the principles for transparent reporting and scientific rigour of preclinical research as stated in the BJP guidelines for Natural Products Research, Design and Analysis, Immunoblotting and Immunochemistry, and Animal Experimentation, and as recommended by funding agencies, publishers and other organisations engaged with supporting research.

Author contributions

Yuanyuan Liu and Wenshan Zhong designed and performed experiments, analyzed data, interpreted the results and wrote the manuscript. Jinning Zhang, Weimou Chen, and Ye Lu performed experiments and analyzed data. Yujie Qiao, Zhaojin Zeng and Haohuang Huang performed experiments. Xiaojing Meng and Fei Zou interpreted the results and edited the manuscript. Hangming Dong and Shaoxi Cai designed and supervised the study, interpreted the results, wrote, and edited the manuscript.

References

Araya J, Kojima J, Takasaka N, Ito S, Fujii S, Hara H, et al.(2013). Insufficient autophagy in idiopathic pulmonary fibrosis. Am J Physiol Lung Cell Mol Physiol 304: L56-69.

Araya J, & Nishimura SJArop (2010). Fibrogenic reactions in lung disease. 5: 77-98.

Baek H, Kim D, Park H, Jang K, Kang M, Lee D, et al. (2012). Involvement of endoplasmic reticulum stress in myofibroblastic differentiation of lung fibroblasts. 46: 731-739.

Bai X, Ma D, Liu A, Shen X, Wang Q, Liu Y, et al. (2007). Rheb activates mTOR by antagonizing its endogenous inhibitor, FKBP38. 318: 977-980.

Barth S, Glick D, & Macleod KF (2010). Autophagy: assays and artifacts. J Pathol 221: 117-124.

Bhagya N, & Chandrashekar KR (2016). Tetrandrine–A molecule of wide bioactivity. Phytochemistry 125: 5-13.

Bian C, Qin WJ, Zhang CY, Zou GL, Zhu YZ, Chen J, et al. (2018). Thalidomide (THD) alleviates radiation induced lung fibrosis (RILF) via down-regulation of TGF-beta/Smad3 signaling pathway in an Nrf2-dependent manner. Free Radic Biol Med 129: 446-453.

Bueno M, Lai Y, Romero Y, Brands J, St Croix C, Kamga C, et al. (2015). PINK1 deficiency impairs mitochondrial homeostasis and promotes lung fibrosis. 125: 521-538.

Ciani B, Layfield R, Cavey J, Sheppard P, & Searle MJTJobc (2003). Structure of the ubiquitin-associated domain of p62 (SQSTM1) and implications for mutations that cause Paget's disease of bone. 278: 37409-37412.

Curtis M, Alexander S, Cirino G, Docherty J, George C, Giembycz M, *et al.* (2018). Experimental design and analysis and their reporting II: updated and simplified guidance for authors and peer reviewers. 175: 987-993.

Hariharan N, Zhai P, Sadoshima JJA, & signaling r (2011). Oxidative stress stimulates autophagic flux during ischemia/reperfusion. 14: 2179-2190.

Hayes J, & McMahon MJTibs (2009). NRF2 and KEAP1 mutations: permanent activation of an adaptive response in cancer. 34: 176-188.

Hu B, Zhang Y, Jia L, Wu H, Fan C, Sun Y, *et al.* (2015). Binding of the pathogen receptor HSP90AA1 to avibirnavirus VP2 induces autophagy by inactivating the AKT-MTOR pathway. 11: 503-515.

Huang J, & Manning BJTBj (2008). The TSC1-TSC2 complex: a molecular switchboard controlling cell growth. 412: 179-190.

Hübner R, Gitter W, El Mokhtari N, Mathiak M, Both M, Bolte H, et al. (2008). Standardized quantification of pulmonary fibrosis in histological samples. 44: 507-511, 514-507.

Ichimura Y, Waguri S, Sou Y, Kageyama S, Hasegawa J, Ishimura R, et al. (2013). Phosphorylation of p62 activates the Keap1-Nrf2 pathway during selective autophagy. 51: 618-631.

Iso T, Suzuki T, Baird L, Yamamoto MJM, & biology c (2016). Absolute Amounts and Status of the Nrf2-Keap1-Cul3 Complex within Cells. 36: 3100-3112.

J H, A F, R H, & journal MTJTEr (2015). Global incidence and mortality of idiopathic pulmonary fibrosis: a systematic review. 46:795-806.

Jiang L, Xu L, Mao J, Li J, Fang L, Zhou Y, et al. (2013). Rheb/mTORC1 signaling promotes kidney fibroblast activation and fibrosis. J Am Soc Nephrol 24: 1114-1126.

King T, Bradford W, Castro-Bernardini S, Fagan E, Glaspole I, Glassberg M, et al. (2014). A phase 3 trial of pirfenidone in patients with idiopathic pulmonary fibrosis. 370: 2083-2092.

Klionsky D, Cuervo A, & Seglen PJA (2007). Methods for monitoring autophagy from yeast to human. 3: 181-206.

Lamark T, Svenning S, & Johansen T (2017). Regulation of selective autophagy: the p62/SQSTM1 paradigm. Essays Biochem 61: 609-624.

Lane JD, Svenning S, & Johansen T (2013). Selective autophagy. Essays in Biochemistry 55: 79-92.

Li S, Fan TP, Jia W, Lu A, & Zhang W (2014). Network pharmacology in traditional chinese medicine. Evid Based Complement Alternat Med 2014: 138460.

Lippai M, & Low P (2014). The role of the selective adaptor p62 and ubiquitin-like proteins in autophagy. Biomed Res Int 2014:832704.

Liu C, Gong K, Mao X, & Li WJIjoc (2011). Tetrandrine induces apoptosis by activating reactive oxygen species and repressing Akt activity in human hepatocellular carcinoma. 129: 1519-1531.

Liu Y, Kern J, Walker J, Johnson J, Schultz P, & Luesch HJPotNAoSotUSoA (2007). A genomic screen for activators of the antioxidant response element. 104: 5205-5210.

Moscat J, & Diaz-Meco MJC (2009). p62 at the crossroads of autophagy, apoptosis, and cancer. 137: 1001-1004.

Narita M, Young A, Arakawa S, Samarajiwa S, Nakashima T, Yoshida S, et al. (2011). Spatial coupling of mTOR and autophagy augments secretory phenotypes. 332: 966-970.

Ohashi A, Ohori M, Iwai K, Nakayama Y, Nambu T, Morishita D, et al. (2015). Aneuploidy generates proteotoxic stress and DNA damage concurrently with p53-mediated post-mitotic apoptosis in SAC-impaired cells. 6: 7668.

Patel AS, Lin L, Geyer A, Haspel JA, An CH, Cao J, et al. (2012). Autophagy in idiopathic pulmonary fibrosis. PLoS One 7: e41394.

Richeldi L, du Bois R, Raghu G, Azuma A, Brown K, Costabel U, et al. (2014). Efficacy and safety of nintedanib in idiopathic pulmonary fibrosis. 370: 2071-2082.

Settembre C, Di Malta C, Polito V, Garcia Arencibia M, Vetrini F, Erdin S, et al. (2011). TFEB links autophagy to lysosomal biogenesis. 332: 1429-1433.

SM G, M H-W, C C, GM vW, M M, L P, et al. (2011). Rheb is essential for murine development. 31: 1672-1678.

Sosulski ML, Gongora R, Danchuk S, Dong C, Luo F, & Sanchez CG (2015). Deregulation of selective autophagy during aging and pulmonary fibrosis: the role of TGFbeta1. Aging Cell 14: 774-783.

Svenning S, & Johansen T (2013). Selective autophagy. Essays Biochem 55: 79-92.

TE K, A P, & M S (2011). Idiopathic pulmonary fibrosis. Lancet (London, England) 378: 1949-1961.

Teng G, Svystonyuk D, Mewhort H, Turnbull J, Belke D, Duff H, et al. (2015). Tetrandrine reverses human cardiac myofibroblast activation and myocardial fibrosis. 308: H1564-1574.

Wang H, Liu T, Li L, Wang Q, Yu C, Liu X, et al. (2015). Tetrandrine is a potent cell autophagy agonist via activated intracellular reactive oxygen species. 5: 4.

Yin M, Lian L, Piao D, & Nan JJWjog (2007). Tetrandrine stimulates the apoptosis of hepatic stellate cells and ameliorates development of fibrosis in a thioacetamide rat model. 13: 1214-1220.

Yu L, McPhee C, Zheng L, Mardones G, Rong Y, Peng J, et al. (2010). Termination of autophagy and reformation of lysosomes regulated by mTOR. 465: 942-946.

Zhang Z, Liu T, Yu M, Li K, & Li W (2018). The plant alkaloid tetrandrine inhibits metastasis via autophagydependent Wnt/beta-catenin and metastatic tumor antigen 1 signaling in human liver cancer cells. J Exp Clin Cancer Res 37: 7.

Figure legends

Figure 1. Τετρανδρινε συππρεσσες ΤΓΦ-β1-ινδυςεδ μψοφιβροβλαστς τρανσδιφφερεντιατιον, προλιφερατιον ανδ E^{*}M δεποσιτιον ιν πριμαρψ MΛΦς. (A) Chemical structure of TET. Its Molecular formation is C38H42N2O6.(B) Primary MLFs were incubated with various indicated concentrations of TET for 24 h and subjected to CCK8 assay to assess cell viability. One-way ANOVA with Dunnett's multiple comparison test: *p < 0.05 comparison to TET=0 µM group value: *p<0.05. (C and D) Primary MLFs were pretreated with DMSO or TET (4 µM) for 1 h and stimulated with or without TGFβ1 (10 ng/ml) for 24 h. Representative immunoblot analysis (C) and quantitative analysis (D) show the expression of ECM deposition (fibronectin, COL-I), myofibroblasts transdifferentiation (vimentin, α-SMA). (E and F) Representative Immunofluorescence monitored by confocal microscopy (E) and quantitative analysis (F) show the expression of α-SMA (red) in Primary MLFs. Blue staining indicates nuclei Scale bars: 100 µM. (G and H) Representative Immunofluorescence (G) and quantitative analysis (H) of EdU -positive cell proportion show the proliferation marker (EdU: 5-ehtynal-2'-deoxyuridine) in myofibroblast. Scale bars: 100 µM. (I-K)Representative immunoblot analysis (I) and quantitative analysis (J and K) show the expression of TGF-β/smad pathway markers (p-smad2, smad2, p-smad3, smad3) in primary MLFs. P values were determined by two-way ANOVA with Tukey's multiple comparison test(n=5): *p<0.05.

Figure 2. Analysis of TET's targets on pulmonary fibrosis based on network pharmacology. (A) Protein-protein interaction (PPI) networks of active ingredients of TET for the treatment of pulmonary fibrosis. Each node represents the relevant genes, the edge means line thickness indicates the strength of data support. (B) Hub top 10 genes in PPI network, the lighter the color, the higher the score; The larger the diameter, the higher the score. (C) Representative networks assembled by predicted TET targets. Diamonds in various colors nodes represent the targets for TET identified through target mapping. Green nodes represent signaling pathways or processes. Targets are connected with pathways or processes with Inner circle in the corresponding color.(D) The GO analysis was discovered with the top 5 enriched conditions in the biological process (BP), cell component (CC), and molecular function (MF) categories. (E) KEGG pathways of target genes.

Φιγυρε 3. TET ρεστορες TΓΦ-β1-ινδυςεδ ιμπαιρεδ αυτοπηαγψ ιν πριμαφψ MΛΦς. (A-C) Primary MLFs were pretreated with TET for indicated concentrations for 1 h and then subsequently stimulated with or without TGF-β1 (10 ng/ml) for 24 h. Representative immunoblot analysis (A) and quantitative analysis (B-C) showed the expression of autophagy (MAP1LC3-I/II, SQSTM1) markers and β-actin (loading control). Values in bar graph are presented as means ± SEM (n=5). Two-way ANOVA: *P < 0.05, **P < 0.01, versus the control group; #p < 0.05, ##p < 0.01, versus the TGF-β1 group.(D) Primary MLFs were pretreated with DMSO or TET (4 µM) for 1 h and stimulated with or without TGF-β1 (10 ng/ml) for 24 h. Representative of qPCR analysis showed the mRNA expression of SQSTM1.(E and F) Primary MLFs were exposed to TGF-β1 (10 ng/ml) for 24h. In some experimental groups, cells were treated with TET (4 µM), 3-methyladenine (3MA: 500 nM). Immunoblot assays (E) and densitometric analysis (F) showed the expression of autophagic markers.(G and H) Primary MLFs were treated with TGF-β1 (10 ng/ml) in the presence/absence of TET (4 µM) or chloroquine (CQ: 20 µM). The protein sample were collected 24 h after the treatment. The levels of autophagic markers were examined with immunoblotting (G). Relative levels of autophagic markers were determined by densitometry and normalized to β -actin levels (H). (I and J)Primary MLFs were treated with TGF- β 1 (0 or 10 ng/ml) for 24 h in the presence/absence of TET (4 μ M), 3MA (500 nM) or CQ (20 μ M). Representative images of immunofluorescence monitored by confocal microscopy (I) and quantification (J) showed the expression of autophagic marker (MAP1LC3B). Green staining is MAP1LC3B, blue staining indicates nuclei. Scale bars: 20 μ m. (K) The transmission electron microscopy images showed numerous double-membraned cytoplasmic vacuolation(arrows). Scale bars: left panels, 5 μ m; right panels, 1 μ m.(L and M) Primary MLFs were transfected with mRFP-GFP-LC3B plasmids for 48h and treated with TGF- β 1 (10 ng/ml) for 24 h in the presence/absence of TET (4 μ M), rapamycin (RAP: 50 nM) or CQ (20 μ M). Representative immunofluorescent images showed mRFP (green), GFP (red) and merged mRFP and GFP (yellow) puncta (L). Scale bars: 10 μ m. Quantification of red (mRFP+ GFP-) and yellow (mRFP+ GFP+) puncta per cell (M). Values in bar graph are presented as means \pm SEM (n=5). Two-way ANOVA with Tukey's multiple comparison test(n=5): *p < 0.05, **p < 0.01, **p < 0.01, **p < 0.01.

Figure 4.TET promotes the interaction of SQSTM1 with MAP1LC3B and with ubiquitinated protein. Primary MLFs were pretreated with TET or DMSO for 1 h and then subsequently stimulated with TGF- β 1 for 24 h. (*A*-*B*)Co-immunoprecipitation (Co-IP) assays with SQSTM1 and MAP1LC3-I/II. Samples before (Input) and after (IP) immunopurification were analyzed by immunoblotting using SQSTM1 and MAP1LC3-I/II antibodies.(*C*) Co-IP assays with SQSTM1 and ubiquitinated protein. Samples were analyzed by immunoblotting using SQSTM1 and ubiquitin (UB) antibodies. (*D*) Confocal microscopy analysis of co-localization of MAP1LC3B and SQSTM1 in primary MLFs. The representative single optical sections and merge images are shown in the right panel. In these representative images, MAP1LC3B is visualized in green, SQSTM1 in red. Scale bars: 10 μ m. (*E*) Confocal microscopy analysis of co-localization of UB and SQSTM1. Scale bars: 10 μ m. UB is visualized in green, SQSTM1 in red.

Figure 5. TET regulates the transcription of SQSTM1 through NRF2. Primary MLFs were treated with TGF- β 1 (0 or 10 ng/ml) for 24 h in the presence/absence of TET (4 μ M). (*A-B*) Immunoblot assays (A) and densitometric analysis (B) showed the expression of NRF2.(*C*) Identification of SQSTM1 promoter-containing genes in the mouse genome by the FIMO software tool. (*D*)Schematic representation of the SQSTM1 promotor region. PCR primers used for amplification (P1 and P2) are shown in the underneath schematic representation. (*E*) ChIP-PCR analysis to showing the association of NRF2 with the SQSTM1 promotor in MLFs.*RT -PCR* products were resolved by agarose gel electrophoresis. (*F*) Statistical analysis was obtained. Values in bar graph are presented as means \pm SEM (n=5). Two-way ANOVA followed by Tukey's multiple comparisons test was used for statistical analysis of (B) and Student's t-test was used for (F). *p < 0.05.

Figure6. TET activates autophagy by inhibiting Rheb/mTORC1 signaling.(A-D) Effect of TET on mTOR activation. Immunoblot (A) and quantitative analysis (B-D) showed the expression level of mTOR phosphorylation (p-mTOR), mTOR downstream substrates (p-P70, p-4E-BP1). (E-F)Representative images of immunofluorescence monitored by confocal microscopy (J) and quantitative analysis (K) showed the expression of p-4E-BP1. Green staining is p-4E-BP1, blue staining indicates nuclei. Scale bars: 20 µm. (G-I) Effect of mTOR activation on autophagy regulation. Primary MLFs were corrected with TET (4 µM) and MHY1485 (5 µM) for 24 h. Immunoblot (G) and quantitative analysis (H-I) showed the expression of autophagy markers (MAP1LC3-I/II, SQSTM1), mTOR activation (mTOR, p-mTOR). (J andK) Effect of TET on the expression of Rheb protein. Representative immunoblot analysis (J) and quantitative analysis (K) show the expression of Rheb protein. (L) Representative of qPCR analysis showed the mRNA expression of Rheb. (M and N) Effect of TET on Rheb activation. Co-immunoprecipitation was performed using agarose beads conjugated to an antibody directed against the GTP γ S and GDP. Immunoblot analysis was performed to check for protein expression of activated Rheb (Rheb/GTP), total Rheb. Total Rheb includes the inactive GDP-Bound form (GDP) and activated Rheb (Rheb/GTP). Values in bar graph are presented as means \pm SEM (n=5). Two-way ANOVA with Tukey's multiple comparison test (n=5). *p < 0.05.

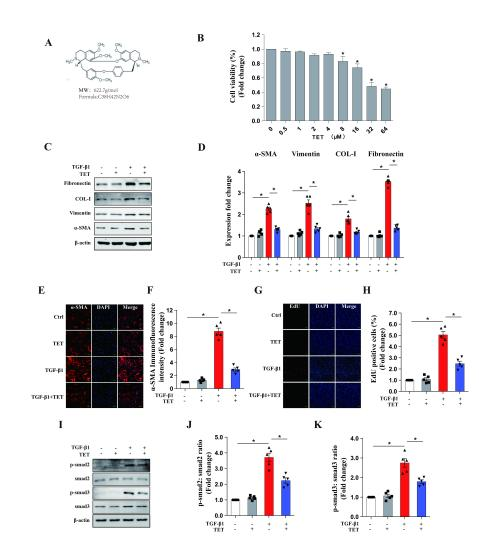
Figure 7. TET improves pulmonary fibrosis by activating autophagy through Rheb/mTOR

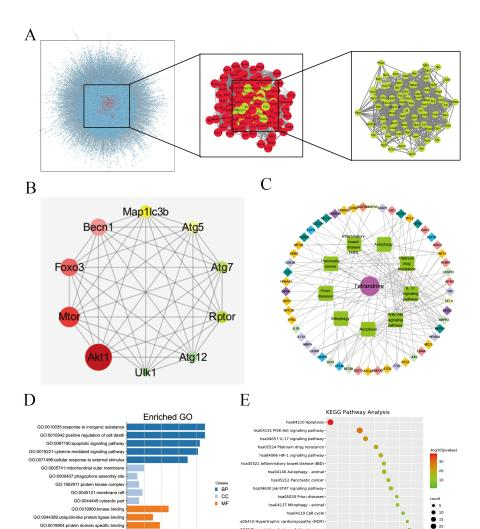
in MLFs. Primary MLFs were treated with TGF- $\beta 1$ (0 or 10 ng/ml) for 24 h in the presence/absence of TET (4 μ M), 3MA (500 nM), RAP (50 nM) or MHY1485 (a small molecule mTOR activator, 5 μ M). (*A* and *B*) Representative immunoblot analysis (A) and quantitative analysis (B) showed the expression of fibrosis-associated proteins.(*C* and *D*) The effect of autophagy on TGF- $\beta 1$ -induced primary MLFs. Immunoblot (C) and quantitative analysis (D) showed the expression of ECM deposition, myofibroblasts transdifferentiation markers. (*E* and *F*) Confocal microscopy images (E) and relative fluorescence intensity of α -SMA (F). α -SMA was visualized in green, DAPI-stained nuclei in blue. Scale bars: 50 μ m. (*G*) MLFs transfected with nonspecific nonsilencing negative siRNA control (*si* -*NC*) or ATG7 small interfering *RNA* (*si* -ATG7) for 48h were treated with TET and TGF- $\beta 1$. Representative immunoblot analysis showed the expression of fibrosis-associated proteins. (*H*) Cells transfected with the empty vector plasmid (vector) or Rheb overexpression plasmid (Rheb) for 48h and then incubated with TET and TGF- $\beta 1$. Immunoblot of fibrosis-associated proteins. (*I*) TET-attenuated fibrosis was associated with mTOR activation. Immunoblot showed the expression of fibrosis-associated proteins. Values in bar graph are presented as means \pm SEM (n=5). Two-way ANOVA with Tukey's multiple comparison test (n=5). *p < 0.05.

Figure 8. Col-I is degraded by autophagy. Primary MLFs treated with DMSO or TET for 1 h and then subsequently simulated with TGF- β 1 for an additional 24 h.(*A*) Confocal microscopy analysis of colocalization of LAMP2 (lysosomal markers, red) and COL-I (green). The representative single optical sections and merge images are shown. Scale bar: 10 µm.(*B*) Confocal microscopy analysis of colocalization of MAP1LC3B (red) and COL-I (green). The representative single optical sections and merge images are shown. Scale bar: 10 µm.(*B*) Confocal microscopy analysis of colocalization of MAP1LC3B (red) and COL-I (green). The representative single optical sections and merge images are shown. Scale bar: 10 µM.(*C*) Co-immunoprecipitation (Co-IP) assays with SQSTM1 and COL-I. Samples before (Input) and after (IP) immunopurification were analyzed by immunoblotting.

Figure 9. TET treatment protects against pulmonary fibrosis induced by bleomycin. Mice, were treated prophylactically with either vehicle (sodium carboxymethyl cellulose, i.p., daily) or TET (20 mg·kg⁻¹·d⁻¹, i.p.) starting on Day 1 after receiving a single intratracheal administration of BLM. The control group received intratracheal PBS. (A) Schematic diagram of the time course of TET treatment in a mouse model of BLM-induced pulmonary fibrosis. (B) Changes in body weight were presented relative to the initial weight. (*C*-*F*) The pulmonary function parameters were measured by pulmonary function test. (G) Lung tissue was sectioned at day 21 and performed HE staining. Scale bar of top images: 100 µm, below images: 40 µm. (H) Lung tissues were stain with Masson trichrome staining. Scale bars: 40 µm. (I) Ashcroft scores were analyzed. (J) Hydroxyproline (HYP) expression of each group by hydroxyproline assay. (K) The protein expression of α -SMA (left images) and fibronectin (right images) in lung sample were examined by immunohistochemical staining. Scale bar of top images: 40 µm. (*L*-*M*) Lung tissues were treated as described in (A) and subjected to immunoblots of fibrosis and autophagy-associated proteins(L) and densitometric analysis was obtained (M). The data were presented as the means \pm SEM (n[?]5). Two-way ANOVA followed by Dunnett's multiple comparisons test was used for statistical analysis. **P* < 0.05.

Figure 10.Underlying mechanism of TET against pulmonary fibrosis through SQSTM1mediated activation of autophagy. See the text for details.





5202 Tr

20 30 ne Numbers

Ge

riptional misregulation in cance hsa04216 Ferroptosis

hsa04728 Dopaminergic synapse

-30

304670 Leukocyte transendothelial migration

GO:0019900:kinase binding :0044389:ubiquitin-like protein ligase bind GO:0019904:protein domain specific bind GO:0008134:transcription factor bind

GO:0005126

-10 -20 Enrichment



